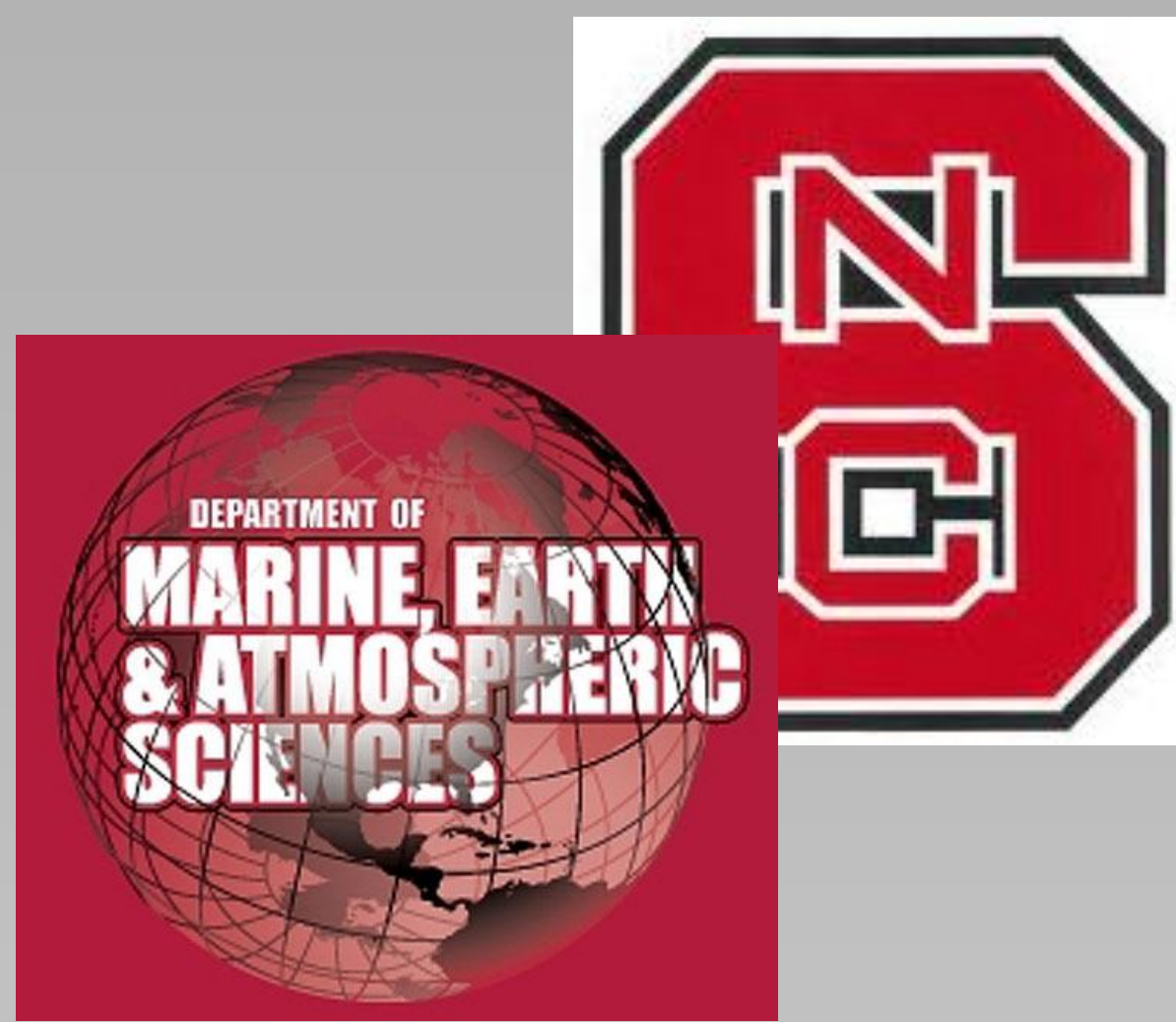


Hurricane Ernesto (2006): Frontal Influence on Precipitation Distribution

Jordan Dale and Gary Lackmann
 North Carolina State University
 Barrett Smith
 NOAA/National Weather Service
 Raleigh, North Carolina

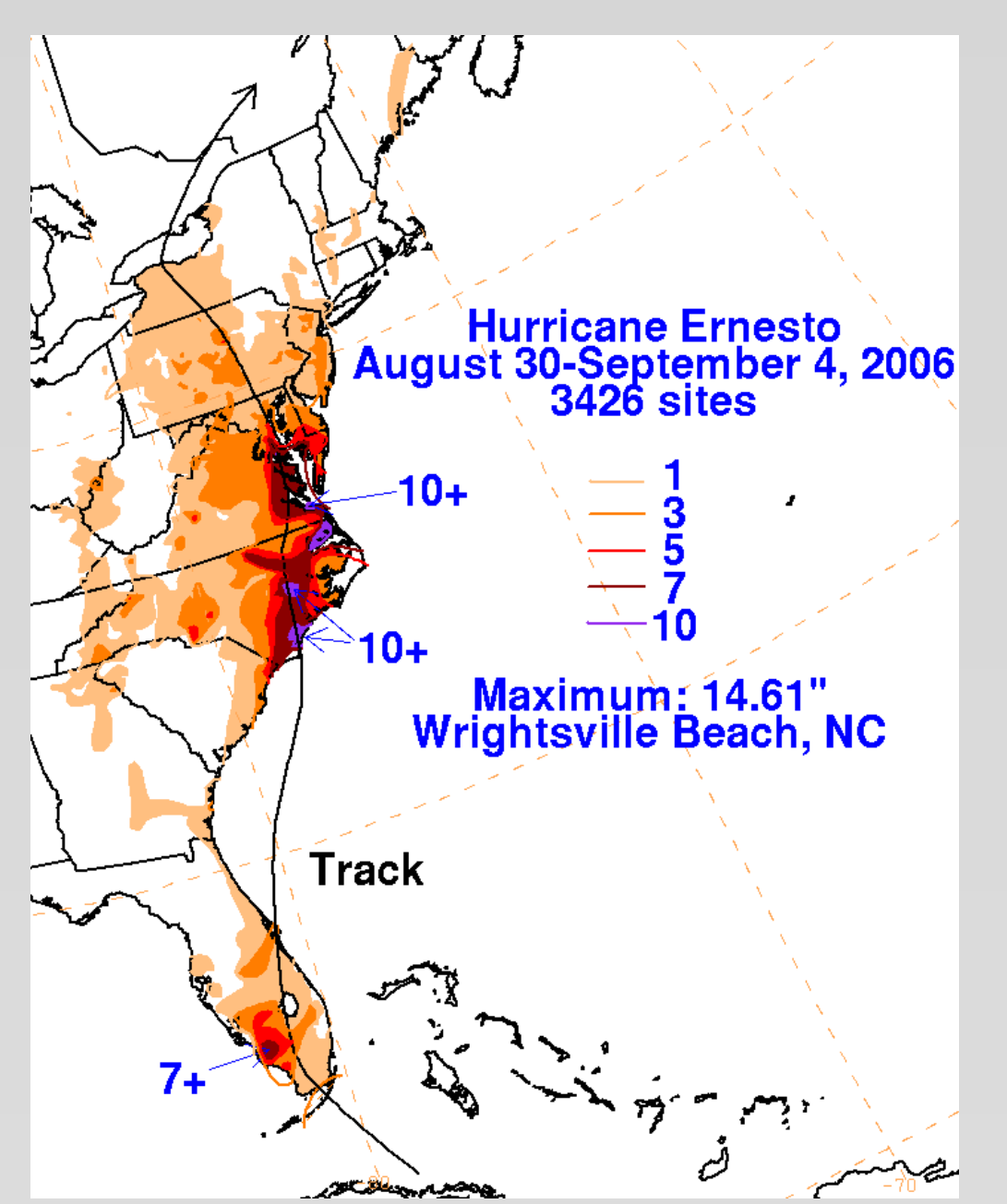


Motivation

- The distribution of precipitation associated with landfalling tropical cyclones remains a critical forecast problem and is dependent on several factors, including:
 - storm motion
 - intensity
 - areal extent
 - synoptic-scale forcing
 - topographical characteristics
 - mesoscale boundaries
- Of these factors, mesoscale boundaries are a prominent forecasting challenge due to the small spatial scales and complex origins.
- The purpose of this study is to isolate the physical processes at play during the interaction of tropical cyclones (TC) and boundaries, and then investigate the predictability and impact on quantitative precipitation forecasts (QPF).
- Hurricane Ernesto (2006) was one such case of boundary interaction that presented forecasting challenges in the Carolinas and Virginia.

Event Summary

- Hurricane Ernesto occurred from 24 August – 4 September, 2006 making a second and final landfall as a strong tropical storm near Long Beach, North Carolina on 1 September.
- A cold front stalled along the coast of North and South Carolina in advance of the second landfall of Ernesto.
- Storm total rainfall accumulations in excess of 10 inches occurred throughout eastern North Carolina and Virginia.

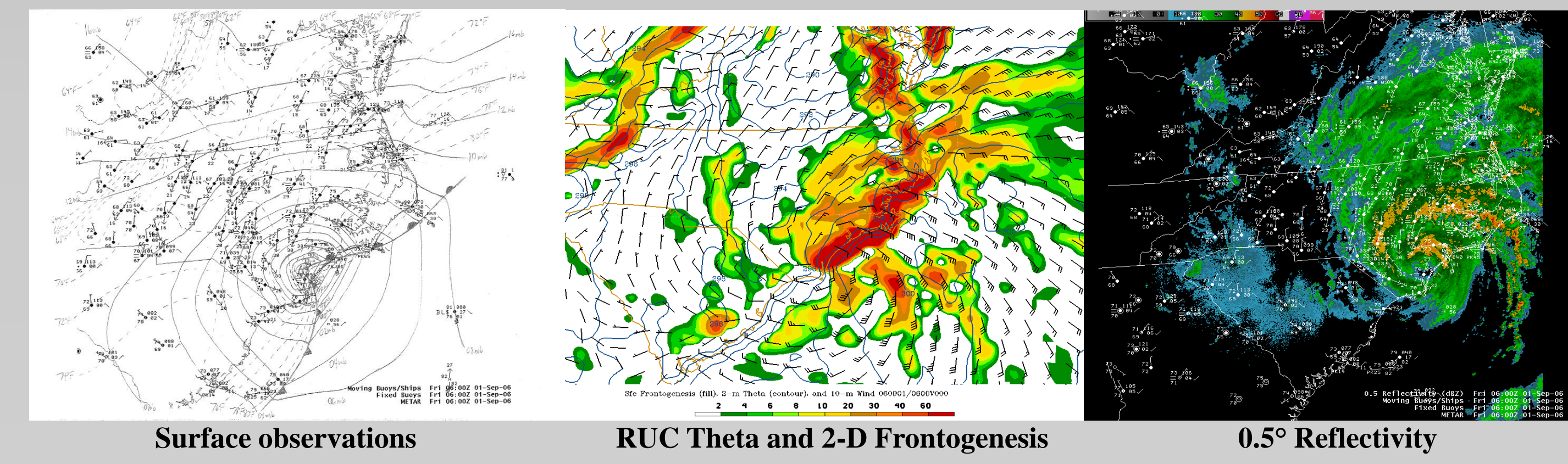


Methods

- The evolution of the frontal boundary was subjectively determined using manual surface analyses, as well as objective analyses of surface 2-D frontogenesis and potential temperature using 20-km RUC data from NCDC.
- The Weather Research and Forecasting Model (WRF) version 3.2.1 was used to produce an ensemble of control runs, using 80-km GFS data from NCDC and 0.7° ECMWF data from NCAR.
- For the most realistic WRF control run, surface 2-D frontogenesis, potential temperature, 850-mb temperature advection, and radar reflectivity were used to isolate the role of the frontal zone in the precipitation distribution.

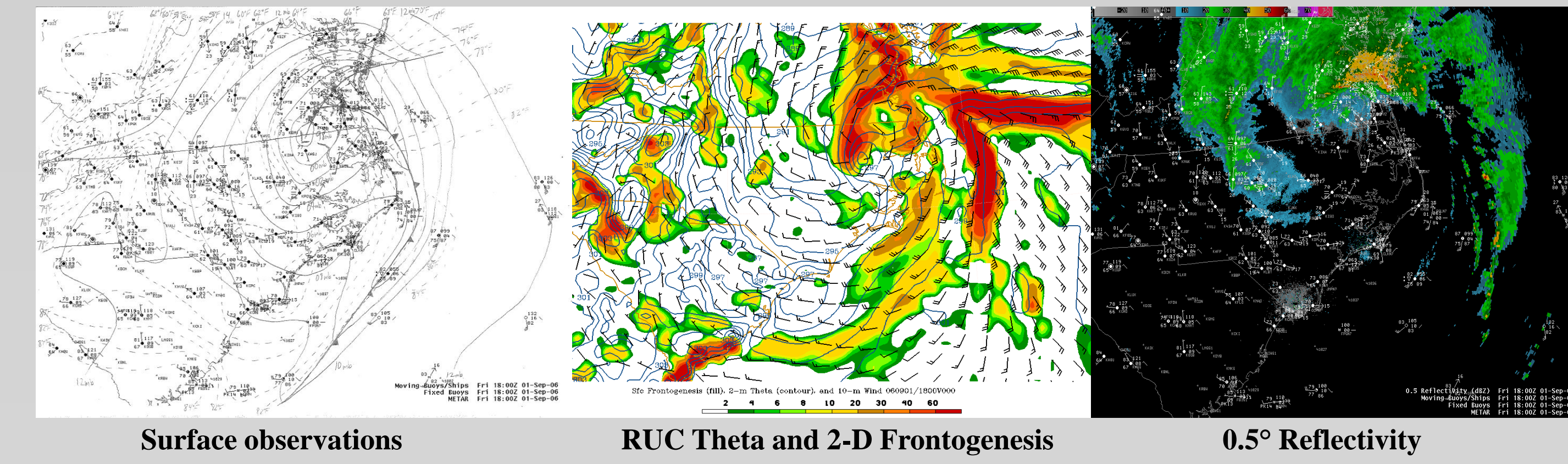
Observational Analysis

0600 UTC 1 September



- A warm front is noted by a theta gradient strong frontogenesis along the coast east of the TC center. A region of enhanced reflectivity is north of the warm front near the TC center.

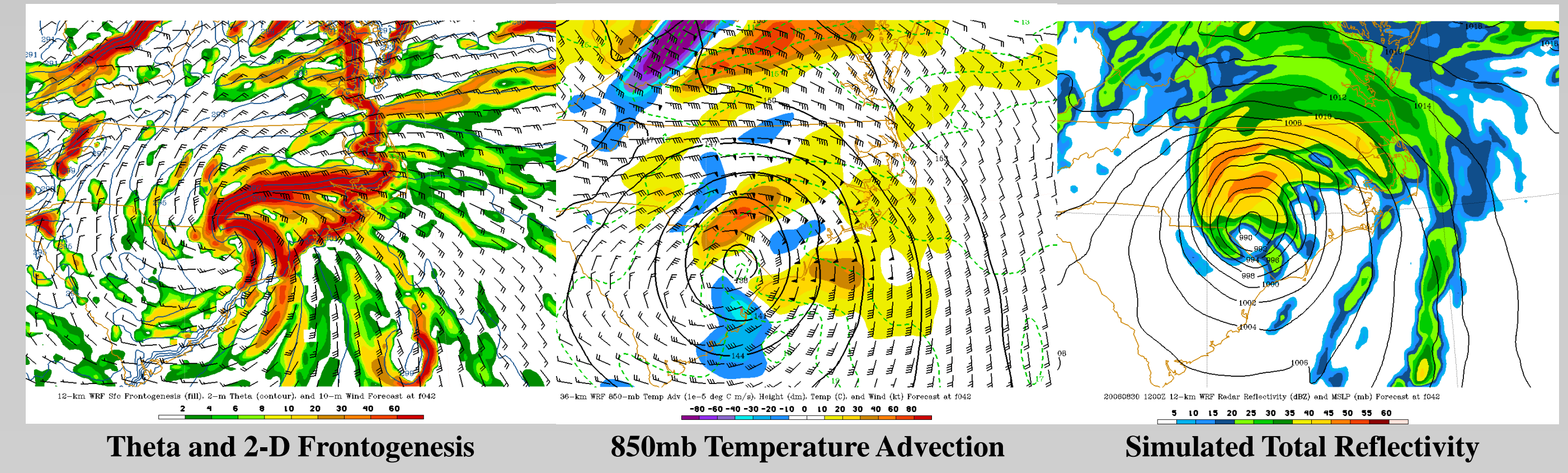
1800 UTC 1 September



- Interaction with the boundary lead to an occluded system with a distinct warm (occluded) front east (north), which is supported by RUC analysis. A region of enhanced reflectivity is located along the occluded and warm fronts ahead of the cold front.

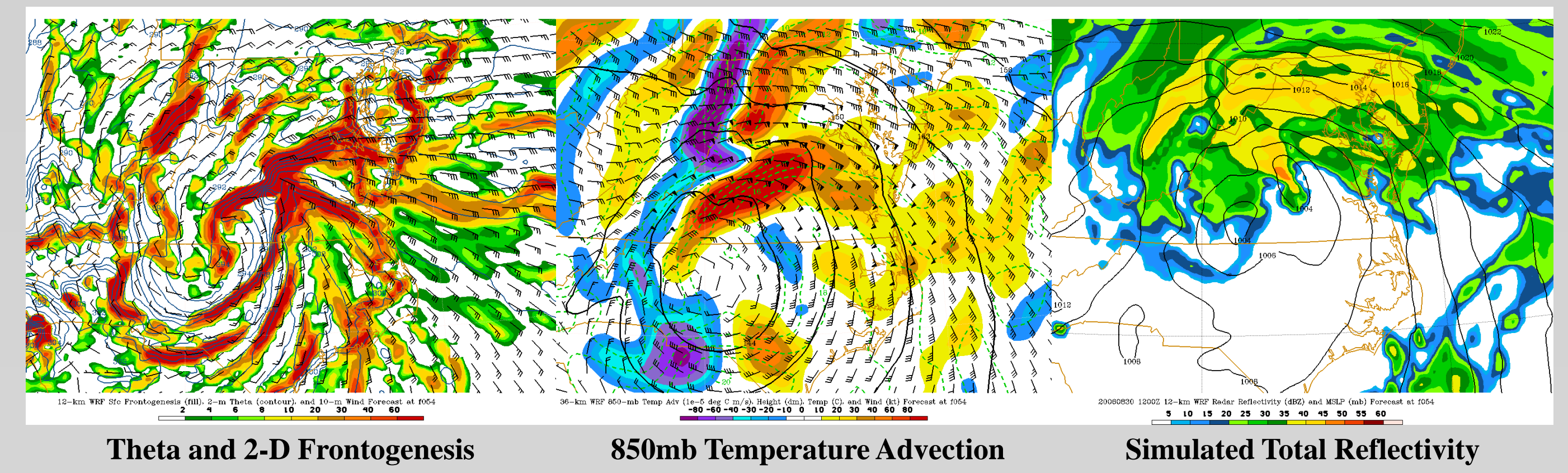
Simulated Frontal Analysis

0600 UTC 1 September



- The locations of frontogenesis and theta gradients with respect to the TC center are similar to observations but displaced westward. Enhanced reflectivities are present to the north of the frontal boundary in locations where 850mb warm advection is occurring.

1800 UTC 1 September

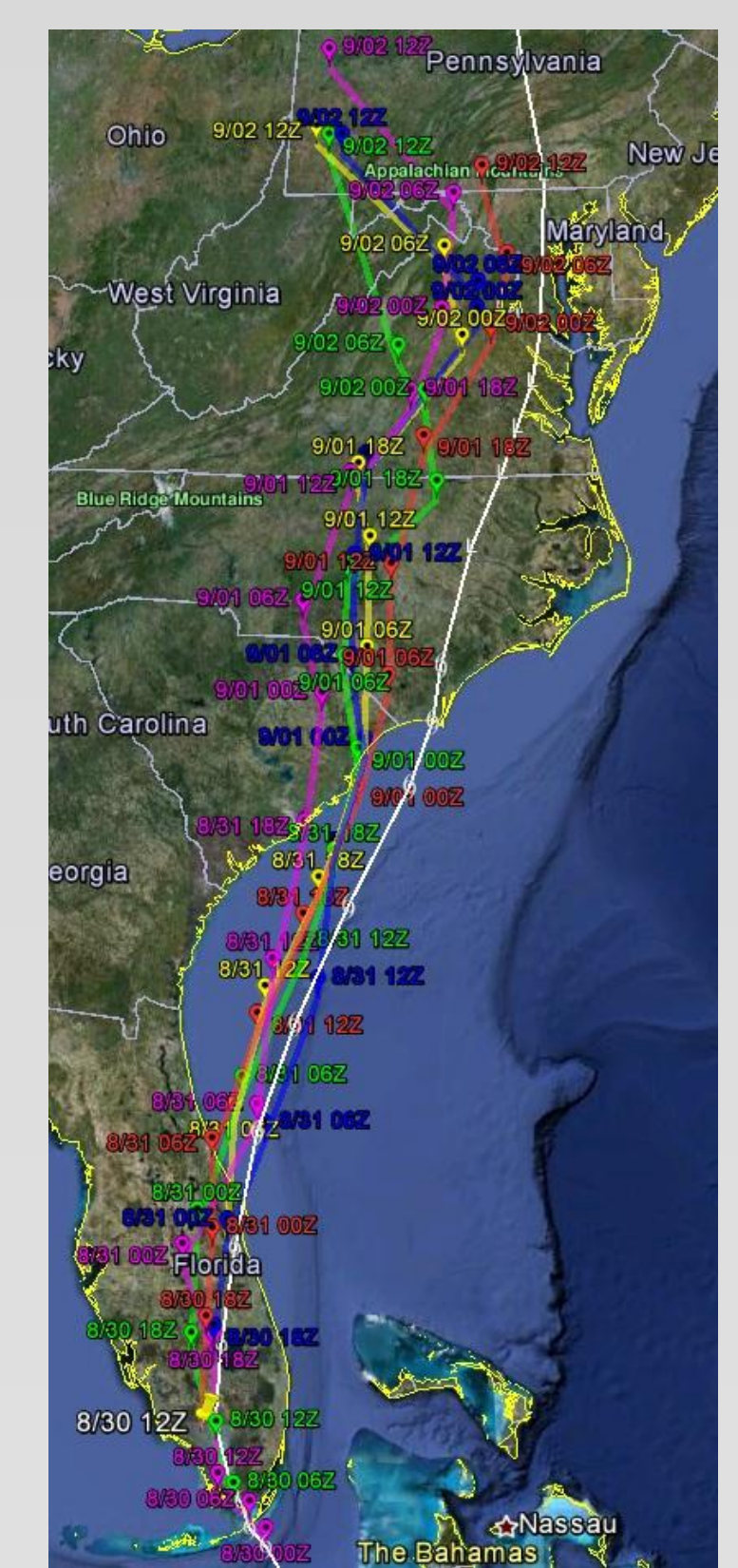


- Frontogenesis and theta gradient concentrated directly north and east of the TC center but displaced westward from observations. Precipitation shield becomes concentrated north of the warm front in a region of strengthening 850mb warm advection (isentropic ascent).

WRF Control Run Ensembles

Model Specifications

- 47 vertical levels up to 50 mb
- WSM 6-class graupel microphysics (MP) scheme
- MYJ TKE boundary layer (BL) scheme
- Noah Land-Surface Model
- BMJ convective parameterization (CP) scheme



GFS Forecast Initialization Runs

White = Best Track
 Purple = 8/30 00Z
 Green = 8/30 06Z
 Red = 8/30 12Z
 Blue = 8/30 18Z
 Yellow = 8/31 00Z

Model Run	Distance RMSE (nmiles)
ECMWF Anl	25.6
GFS Anl f000	25.6
GFS 8/30 12Z Fx	40.9
WRF 36-km 8/30 12Z GFS Fx	50.4
WRF 12-km ECMWF Anl	52.1
WRF 36-km ECMWF Anl	63.8
WRF 8/30 06Z GFS Fx	70.2
WRF 8/30 18Z GFS Fx	73.5
WRF 8/31 00Z GFS Fx	81.9
WRF 4-km 8/30 12Z GFS Fx	86.5
WRF 4-km ECMWF Anl	87.0
WRF 8/30 00Z GFS Fx	88.2
WRF GFS Anl	97.4
WRF 8/30 12Z GFS Fx KF CP	107.9
WRF 12-km 8/30 12Z GFS Fx	109.3
WRF 8/30 12Z GFS Fx GCE MP	118.9

Model Run	MSLP RMSE (mb)
WRF GFS Anl	3.4
WRF 36-km 8/30 12Z GFS Fx	3.6
WRF 8/30 12Z GFS Fx GCE MP	3.8
WRF 8/31 00Z GFS Fx	3.9
WRF 12-km 8/30 12Z GFS Fx	4.2
WRF ECMWF Anl GCE MP	4.5
WRF 8/30 12Z GFS Fx KF CP	4.5
WRF 12-km ECMWF Anl	4.7
WRF 8/30 00Z GFS Fx	4.7
WRF 8/30 18Z GFS Fx	5.0
WRF 36-km ECMWF Anl	5.0
WRF 8/30 06Z GFS Fx	5.2
WRF 4-km ECMWF Anl	6.0
WRF 4-km 8/30 12Z GFS Fx	6.8
GFS Anl f000	7.2
ECMWF Anl	7.5
GFS 8/30 12Z Fx	8.8

- WRF run using initial and lateral boundary conditions from 8/30 12Z GFS Forecast (Fx) data best simulated the track and intensity.

Future Work

What processes or factors contributed most to forecast uncertainty and ensemble spread?

- Weak cold-air damming (CAD) occurred on 31 August. Sensitivity of the TC track to CAD will be tested using numerical simulations.
- A predecessor rainfall event (PRE) occurred on 30 August. The significance of TC-related moisture in the PRE event will be examined using numerical simulations. Additionally, sensitivity of the TC track to the PRE will be investigated.
- Other processes possibly enhancing precipitation along and north of the frontal boundary east of the TC center will be investigated using numerical simulations.
- Other cases involving TC boundary interaction in the Carolinas will be investigated to determine the role of frontal boundaries in modulating TC precipitation distribution.

Acknowledgements

The authors would like to thank Jonathan Blaes, Jim Hudgins, Frank Alsheimer, Eric Seymour, and David Roth for their input on this research. Support for this research is provided by NOAA Collaborative Science, Technology, and Applied Research (CSTAR) Award NA10NWS4680007.